JCTC Journal of Chemical Theory and Computation

Revisiting Molecular Dissociation in Density Functional Theory: A Simple Model

David G. Tempel,[§,†] Todd J. Martínez,[‡] and Neepa T. Maitra*,[†]

Department of Physics and Astronomy, Hunter College and City University of New York, 695 Park Avenue, New York, New York 10065, and Department of Chemistry and The Beckman Institute, University of Illinois, Urbana, Illinois 61801

Abstract: A two-electron one-dimensional model of a heteroatomic molecule composed of two open-shell atoms is considered. Including only two electrons isolates and examines the effect that the highest occupied molecular orbital has on the Kohn−Sham potential as the molecule dissociates. We reproduce the characteristic step and peak that previous high-level wave function methods have shown to exist for real molecules in the low-density internuclear region. The simplicity of our model enables us to investigate in detail their development as a function of bond-length, with little computational effort, and derive properties of their features in the dissociation limit. We show that the onset of the step is coincident with the internuclear separation at which an avoided crossing between the ground-state and lowest charge-transfer excited-state is approached. Although the step and peak features have little effect on the ground-state energetics, we discuss their important consequences for dynamics and response.

I. Introduction

The unprecedented balance between accuracy and efficiency of density functional theory (DFT)[1−5] is in large part the result of the discoveries of John Perdew. The mapping of the true system of interacting electrons to a fictitious one in which the electrons do not interact, yet reproduce the true electron density, requires accurate approximations for the exchange-correlation (xc) potential, which remained elusive until the developments in the 1980's of Perdew and co-workers. Understanding and incorporating exact conditions and physical principles underlie the robustness and reliability of Perdew's functionals. In this spirit, we study here the structure of the exact xc potential as a molecule dissociates, whose landscape of steps and peaks Perdew was one of the first to explore.

In DFT, one solves self-consistently the Kohn−Sham (KS) single-particle equations

$$\left(-\frac{1}{2}\nabla^2 + v_S[\rho](\mathbf{r})\right)\phi_i(\mathbf{r}) = \epsilon_i\phi_i(\mathbf{r}) \tag{1}$$

where $v_S[\rho](\mathbf{r})$ is the KS potential, a functional of the ground-state electronic density, ρ. (Atomic units, $e^2 = \hbar = m_e = 1$, are used throughout this paper). It is usually written as the sum $v_S[\rho](\mathbf{r}) = v_{ext}[\rho](\mathbf{r}) + v_H[\rho](\mathbf{r}) + v_{XC}[\rho](\mathbf{r})$, where $v_{ext}(\mathbf{r})$ is the potential due to the nuclei, $v_H(\mathbf{r}) = \int d^3\mathbf{r}'\rho(\mathbf{r}')/|\mathbf{r} - \mathbf{r}'|$ is the classical Hartree potential and $v_{XC}(\mathbf{r})$ is the exchange-correlation (xc) potential, incorporating the remaining many-body effects in a one-body potential. The KS orbitals ϕ_i yield the true density according to

$$\rho(\mathbf{r}) = \sum_{i=1}^{N}\phi_i(\mathbf{r})^2 \tag{2}$$

In principle, the ground-state density and all static properties of the true interacting system are exactly recovered, but in practice approximations are needed for the unknown xc potential $v_{xc}[\rho]$ as a functional of the density. Typically, semilocal functionals, such as GGA's[6] and meta-GGA's[7,8] give good energies and structural properties at equilibrium

* To whom correspondence should be addressed. E-mail: nmaitra@hunter.cuny.edu

† Department of Physics and Astronomy, Hunter College and City University of New York.

‡ Department of Chemistry and The Beckman Institute, University of Illinois.

§ Present address: Department of Physics, Harvard University, 17 Oxford Street, Cambridge, MA 02138.

Molecular Dissociation in DFT

J. Chem. Theory Comput., Vol. 5, No. 4, 2009 **771**

molecular geometries; the nonempirical constructions of Perdew and co-workers impart a reliability to the description of diverse systems and properties. However, GGA's do not perform so well for weakly coupled subsystems. Notably, recent work has been very successful in describing van der Waal's forces using sophisticated nonlocal approximations in DFT.[9−11] For molecules dissociating into open-shells, the failure of semilocal approximations becomes drastic, yielding unphysical fractional charges on the separated species.[12−15] This problem was first highlighted by Perdew,[13,14] motivated by the observation of Slater[12] that his "$X\alpha$" method yields a similar result.

Figure 7 of ref 14 shows that the exact xc potential develops a "region of positive constant" around the atom with the "tighter density distribution", in the limit of infinite separation, using a simple one-dimensional model. More generally, the effect of molecular dissociation on the ground-state xc potential for the case of real diatomic closed-shell molecules consisting of open shell atoms has been studied systematically, by Baerends, Gritsenko, and co-workers, in a series of papers.[16−21] In ref 16, the simplest case of this, the two-electron H_2 molecule was studied. The absence of long-range left-right correlation in Hartree−Fock, renders its potential overly repulsive near the nuclei, leading to an overly diffuse density. A highly accurate xc potential was constructed from correlated CISD first- and second- order density matrices in ref 16, and the resulting correlation potential was shown to considerably reduce the repulsion at the nuclei. It was also shown that the xc potential develops a sharp maximum (peak) at the bond midpoint. A very thorough analysis of the KS potential in stretched H_2 was performed later in ref 21, where the effect of different approximate constructions for the KS orbital was investigated and explained in detail (see also section IVB). Using an iterative method introduced in ref 22, the authors of ref 17 were the first to construct molecular KS potentials for more than two electrons from correlated densities. They studied LiH (and H_2) and found significant differences with the local density approximation (LDA) at large separations. The authors of ref 19 calculated the xc potential for the mono-hydrides XH (X = Li, B, F), analyzing its structure via a decomposition or "partitioning" of v_{XC} into various "energy" and "response" components related to the electronic structure.[16,18,20] It was shown that left-right correlation leads to a build-up in the xc potential around the H atom (a "step", as was observed in the simple model of ref 14). The peak present in the bond midpoint of H_2 was found, in the case of the monohydrides, to shift toward the H atom while becoming significantly smaller because of the presence of core electrons softening the left-right correlation effects. The partitioning scheme (reviewed in section II), which had earlier been used to examine atomic xc potentials,[18,20] proved to be a particularly useful tool in the analysis, providing insight into the origin of the peak and step structures.

Molecular dissociation in DFT is particularly relevant when considering time-dependent processes and nuclear dynamics on potential energy surfaces. The advent of time-dependent density functional theory (TDDFT)[23−25] allows for a density-functional description of full electron dynamics and here accurate long-range potentials are an important ingredient for many applications, for example, photodisso-ciation dynamics, excitations in large molecules, including charge-transfer, and molecular transport. A recent paper[26] discussed promising aspects, as well as challenges, in getting accurate excited energy surfaces from TDDFT; certainly it is important to get the ground-state potential energy surface correct.

In the present paper, we study the xc potential of a dissociating closed-shell heteroatomic molecule consisting of two open-shell atoms by analyzing a simple one-dimensional model of two different "one-electron atoms". The two "electrons" and two "nuclei" interact via soft-Coulomb interactions with the softening parameters chosen to approximate certain properties of the real LiH molecule. This simple model allows numerically exact solution at a wide range of separations with little computational effort, while reproducing the essential features, from the point of view of molecular dissociation, of the xc potential for real three-dimensional molecules. It allows some analytic treat-ment of these features that yields further insight into the "step" and "peak" structures mentioned above; for example, predicting the asymptotic height and position of the peak and an explanation of why such a structure, that hardly affects the energetics, must be there. A detailed examination of the stretched bond-length where the step begins to appear, reveals a correlation with the position of the avoided crossing between the ground-state and lowest charge-transfer states. We explain why.

A two-electron model isolates the effects caused by the valence electrons, which play the major role in dissociative processes, without additional potential-features arising from core electrons. In the KS description of dissociation, the major role is played by the KS HOMO, which in the case of open-shell fragments, is delocalized across the molecule. By including only the HOMO in our model, we isolate and examine effects on the dissociating potential energy surface caused solely by this most important orbital. The model is presented in section III, while section IV contains the numerical and analytic results.

We may draw conclusions from this simple model about real three-dimensional molecules composed of open-shell fragments of general odd electron-number, but with a little caution: we find quantitative differences resulting from the lack of core electrons in our model and the much longer effective range of the soft-Coulomb interaction in 1D compared to the true 3D Coulomb interaction. The soft-Coulomb interaction is used in many interesting investiga-tions of strong-field dynamics[27−32] and, recently, in the context of TDDFT:[33,34] these models capture the essence of phenomena such as nonsequential double-ionization, and laser-induced electron-recollision. The peak and step are challenging features for approximations to capture and are lacking in almost all functionals used today. Being in a low-density region, the peak structure has negligible energetic consequence; however it does play a role when response or full dynamics is considered: for example, it reduces the (hyper-)polarizability of long-chain systems.[35] Because they represent barriers to electron transport, the work here is also

relevant to one-dimensional transport calculations in molecular wires,[36] although this fact has not been discussed before, so perhaps not yet been fully appreciated. The step structure, essential to avoid the fractional charge problem, has severe consequences for the structure of the TDDFT xc kernel as we discuss in section V.

II. Decomposition of the xc Potential

The partitioning of the xc potential[16−20] was motivated by first decomposing the xc energy components into "potential" and "kinetic" terms of the form:

$$
\begin{aligned}
E_{xc}[\rho] &= W_{xc}[\rho] + T_c[\rho] \qquad \text{where} \\
W_{xc}[\rho] &= \frac{1}{2}\int \rho(\mathbf{r})v_{xc}^{hole}[\rho](\mathbf{r})d^3r \quad \text{and} \\
T_c[\rho] &= \int \rho(\mathbf{r})v_c^{kin}[\rho](\mathbf{r})
\end{aligned}
\tag{3}
$$

implicitly define hole and correlation kinetic potentials, v_{xc}^{hole} and v_c^{kin}. The total xc potential is then partitioned into three components

$$
v_{xc}[\rho](\mathbf{r}) = v_{xc}^{hole}[\rho](\mathbf{r}) + v_{c,kin}[\rho](\mathbf{r}) + v_{resp}[\rho](\mathbf{r}) \tag{4}
$$

$v_{xc}^{hole}[\rho](\mathbf{r})$ is the Coulomb potential of the xc hole

$$
v_{xc}^{hole}(\mathbf{r}) = \int \frac{\rho_{xc}(\mathbf{r}, \mathbf{r}_2)}{|\mathbf{r} - \mathbf{r}_2|}d^3\mathbf{r}_2 \tag{5}
$$

where the xc hole $\rho_{xc}(\mathbf{r}_1, \mathbf{r}_2)$ is defined through the pair density $P(\mathbf{r}_1, \mathbf{r}_2)$ (joint probability of finding an electron at $\mathbf{r}_1$ while another is at $\mathbf{r}_2$), via $P(\mathbf{r}_1, \mathbf{r}_2) = \rho(\mathbf{r}_1)(\rho(\mathbf{r}_2) + \rho_{xc}(\mathbf{r}_1, \mathbf{r}_2))$. When added to the Hartree potential, $v_{xc}^{hole}(\mathbf{r}) + v_H(\mathbf{r})$ represents the average repulsion an electron at position $\mathbf{r}$ experiences caused by the other (N-1) electrons in the system. In terms of the conditional probability amplitude, whose square gives the probability of finding the other (N-1) electrons in the system with space-spin coordinates $\mathbf{x}_2$, $\mathbf{x}_3,..., \mathbf{x}_N$ when an electron is known to be at position $\mathbf{r}_1$

$$
\Phi(s_1, \mathbf{x}_2, ..., \mathbf{x}_N|\mathbf{r}_1) = \frac{\Psi(\mathbf{x}_1, \mathbf{x}_2, ..., \mathbf{x}_N)}{\sqrt{\dfrac{\rho(\mathbf{r}_1)}{N}}} \tag{6}
$$

where $\Psi(\mathbf{x}_1, \mathbf{x}_2,..., \mathbf{x}_N)$ is the interacting many-electron wave function, we have

$$
\begin{aligned}
v_{xc}^{hole}(\mathbf{r}) + v_H(\mathbf{r}) = \int \Phi^*(s_1, \mathbf{x}_2, ..., \mathbf{x}_N|\mathbf{r}) \times \\
\left[\sum_{i=2}^{N} \frac{1}{|\mathbf{r} - \mathbf{r}_i|}\right]\Phi(s, \mathbf{x}_2, ..., \mathbf{x}_N|\mathbf{r})ds_1 d\mathbf{x}_2...d\mathbf{x}_N \quad (7)
\end{aligned}
$$

The second term in eq 4, $v_{c,kin}[\rho](\mathbf{r})$, is the correlation contribution to the kinetic component of the xc potential. It is the difference of the kinetic components of the interacting and noninteracting KS systems

$$
v_{c,kin}(\mathbf{r}) = v_{kin}(\mathbf{r}) - v_{s,kin}(\mathbf{r}) \tag{8}
$$

where the kinetic components may be written in terms of the conditional probability amplitude

$$
\begin{aligned}
v_{kin}(\mathbf{r}_1) &= \frac{1}{2}\int |\nabla_1 \Phi(s_1, \mathbf{x}_2, ..., \mathbf{x}_N|\mathbf{r}_1)|^2 ds_1 d\mathbf{x}_2...d\mathbf{x}_N \\
&= \frac{\nabla_{1'}\nabla_1 \rho(\mathbf{r}_1', \mathbf{r}_1)^2 \Big|_{\mathbf{r}_1 = \mathbf{r}_1'}}{\rho(\mathbf{r}_1)} - \frac{[\nabla\rho(\mathbf{r}_1)]^2}{8\rho(\mathbf{r}_1)^2}
\end{aligned}
\tag{9}
$$

and

$$
\begin{aligned}
v_{s,kin}(\mathbf{r}_1) &= \frac{1}{2}\int |\nabla_1 \Phi_s(s_1, \mathbf{x}_2, ..., \mathbf{x}_N|\mathbf{r}_1)|^2 ds_1 d\mathbf{x}_2...d\mathbf{x}_N \\
&= \frac{1}{2}\sum_{i=1}^{N}\left|\nabla_1 \frac{\phi_i(\mathbf{r}_1)}{\rho^{1/2}(\mathbf{r}_1)}\right|^2
\end{aligned}
\tag{10}
$$

In eq 9, $\rho(\mathbf{r}_1', \mathbf{r}_1)$ is the first-order spin-summed reduced density-matrix, and in eq 10, $\Phi_s(s_1, \mathbf{x}_2,..., \mathbf{x}_N|\mathbf{r}_1)$ is the conditional probability amplitude of the KS system, which is defined as in eq 6 but with the KS single Slater determinant, whose orbitals are $\phi_i(\mathbf{r})$, replacing the full many-electron wave function.

The final term in eq 4 is the so-called response potential. It may be further partitioned into terms representing the response of the xc hole and the response of the correlation kinetic potential,[18,19] but we will not pursue this further decomposition here.

For two electrons in a spin-singlet, many of these expressions simplify considerably, as the KS single-Slater determinant consists of one doubly occupied spatial orbital, $\phi_0(\mathbf{r})$, which is equal to square root of half the density

$$
\phi_0(\mathbf{r}) = \sqrt{\frac{\rho(\mathbf{r})}{2}} \tag{11}
$$

Substituting into eq 1, we can solve explicitly for the KS potential as a functional of the density

$$
v_S[\rho](\mathbf{r}) = \frac{\nabla^2\sqrt{\rho(\mathbf{r})}}{2\sqrt{\rho(\mathbf{r})}} - I \tag{12}
$$

where I is the first ionization potential of the system. From eq 10, $v_{s,kin}(\mathbf{r}) = 0$ and eq 8 reduces to

$$
v_{c,kin}(\mathbf{r}) = v_{kin}(\mathbf{r}) \tag{13}
$$

Also, for two electrons, $v_x(\mathbf{r}) = v_x^{hole}(\mathbf{r}) = -(1/2)v_H(\mathbf{r})$. The exchange component to the response potential, v_{resp} is zero. We may therefore write

$$
v_x(\mathbf{r}) = -v_H(\mathbf{r})/2 = v_x^{hole}(\mathbf{r}) \tag{14}
$$

$$
v_c(\mathbf{r}) = v_c^{hole}(\mathbf{r}) + v_{c,kin}(\mathbf{r}) + v_{c,resp}(\mathbf{r}) \tag{15}
$$

As was found in refs 18 and 19, as a heteroatomic molecule dissociates, a step structure in the low-density bond midpoint region arises in the response component, v_{resp}, accompanied by a peak structure in the kinetic component $v_{c,kin}$ of the xc potential (see also Figures 3 and 4).

Consider now a simplified description of the molecule that has includes just one electron on each atom. As explained in ref 16 and reflected in eq 9, $v_{kin}(\mathbf{r})$ depends on the gradient of the conditional probability amplitude, so describes how

Molecular Dissociation in DFT

J. Chem. Theory Comput., Vol. 5, No. 4, 2009 **773**

strongly the motion of an electron at reference position **r** is correlated with the other electrons in the system. For **r** near one of the nuclei, the reference electron moves in a potential dominated by the nuclear potential, the conditional amplitude Φ reduces to the atomic HOMO of the other atom, and does not change for small changes around **r**; hence v_{kin} goes to zero. But in the internuclear region, the motion of the two electrons becomes correlated: as the reference position moves from one nucleus to the other, the conditional probability of finding the other switches from being toward one atom to the other, and so v_{kin} peaks.

The origin of the step structure was also analyzed extensively in ref 19 and shown to arise in the correlation component of the response potential, v_c^{resp}. It was discovered earlier,[14,39] in relation to the derivative discontinuity,[13,14,39,40] that the correlation potential for a long-range molecule composed of two open-shell atoms must have a step in the midpoint region, whose size is such that the atomic HOMO orbital energies realign. From Koopman's theorem, the HOMO energy equals the ionization potential; therefore the step has a size $\Delta I = I_2 - I_1$, where $I_{2,1}$ is the larger(smaller) ionization potential of the two atoms, raising the potential of the more tightly bound atom. Far away from the molecule the potential near this atom steps back down to zero. A simple way to understand the origin of the step is to realize that had the step not been there, then one could lower the ground-state energy of the long-range molecule by transferring a fraction of charge from the atom with the higher ionization potential to that with the lower, leading to the molecule dissociating into fractionally charged species. Because this cannot happen, the KS potential develops a step in the bonding region, which realigns the atomic HOMOs, so preventing any bias. Another way to put this is that the chemical potential must be the same throughout the long-range molecule and equal to the molecular HOMO orbital energy. Since the chemical potential of the true system is the smallest ionization potential in the system at infinite separation, the KS potential near the atom with the larger atomic ionization potential must be uniformly raised by ΔI to bring it to the ionization potential of the other atom, while asymptotically stepping back down to zero.

We shall now introduce our two-electron model to study these features further and how they develop as a function of bond-length.

III. A One-Dimensional Two-Electron Model of LiH

A simple one-dimensional, two-electron model of lithium hydride can be used to illustrate several important features of heteroatomic dissociation. Much of the essential physics of the dissociation process may be captured by focusing on the chemically important valence electrons, while representing the effect of the core electrons by an average effective potential, such as a pseudopotential or frozen-core approximation. In the case of LiH, the two core electrons are localized in the Li 1s shell, while the two valence electrons are delocalized across the molecule. Our goal is to analyze the effect of bond breaking and formation on the various xc components (eq 4), which in a real molecule will be partially

obscured by shell structure and other many-electron effects from the electrons in the Li 1s core. Our two-electron model enables us to circumvent this complication, by focusing solely on the electrons involved in the bond, and their effect on the Kohn–Sham characteristics. As further simplication, it is reasonable to use a one-dimensional model, where the coordinate is taken to be along the bond axis, for cylindrically symmetric systems such as a diatomic molecule.

As is often done in one-dimensional models, the Coulomb potential $\pm 1/|\mathbf{r} - \mathbf{r}'|$ is replaced by a soft-Coulomb potential, $\pm 1/[a + (x - x')^2]^{1/2}$. For a model of LiH at interatomic separation R, we write the electron–nuclear potential as

$$v_{ext}(x) = -\frac{1}{\sqrt{a + (x - R/2)^2}} - \frac{1}{\sqrt{b + (x + R/2)^2}} \quad (16)$$

The "softening parameters" a and b are directly related to the ionization potentials of the individual atoms (see shortly). Similarly, the electron–electron repulsion is represented by a soft-Coulomb form

$$v_{ee}(x_1, x_2) = \frac{1}{\sqrt{c + (x_1 - x_2)^2}} \quad (17)$$

We place Li at $-R/2$ and H at $R/2$, and choose the parameters $a = 0.7$, $b = 2.25$, and $c = 0.6$, for reasons explained in the following. With $a = 0.7$, the ionization potential of hydrogen in our model comes out to be 0.776H as compared with 0.5H for the real atom. Taking $b = 2.25$ yields that of Li in our model as 0.476H as compared with 0.198H for the real lithium atom. The correct difference in ionization potentials of the atoms $\Delta I = I_H - I_{Li} = 0.3$H is however exactly reproduced by our parameters; ΔI is a key quantity in our analysis of the KS potential at large interatomic separations. Because of the long-range nature of the soft-Coulomb interaction, we choose the atomic ionization potentials be larger than in the true 3D case to prevent the atomic densities of the individual atoms from being too diffuse. Other factors considered were the equilibrium bond length (model 1.6 au, true 3.0 au), dissociation energy (model 0.068H, true 0.092H) and molecular first ionization potential (model 0.51H, true 0.29H), where the nuclear–nuclear interaction is modeled by

$$v_{nn}(R) = \frac{1}{\sqrt{(a + b - c) + R^2}} \quad (18)$$

In Figure 1, the dissociation curve for our model is plotted for comparison with that of 3D LiH.[41]

IV. Numerical Solution and Results

We use a standard Runge–Kutta differential equation solver, as implemented in the octopus code,[42–44] to numerically solve for the ground-state wave function $\Psi(x, x')$ of the Hamiltonian:

$$H = -\frac{1}{2}\frac{d^2}{dx_1^2} - \frac{1}{2}\frac{d^2}{dx_2^2} + v_{ext}(x_1) + v_{ext}(x_2) + v_{ee}(x_1 - x_2) \quad (19)$$

where $v_{ext}(x)$ and $v_{ee}(x_1 - x_2)$ are defined in eqs 16 and 17. The above two particle Hamiltonian is mathematically equivalent to that of one particle moving in the two-dimensional potential[42−44]

$$v_{ext}(x) + v_{ext}(y) + v_{ee}(x - y) \qquad (20)$$

We solve the equivalent one-particle Schrödinger equation on a rectangular two-dimensional 25 by 25 au real space grid. The grid points are separated by a distance of 0.04 au.

The density is obtained from the wave function through $\rho(x) = 2\int dx' |\Psi(x, x')|^2$ and then substituted into eq 12 to yield the exact KS potential. The xc potential can be isolated from subtracting the external potential eq 16 and the Hartree potential, $v_H(x) = \int \rho(x) v_{ee}(x - x') dx'$ (using v_{ee} from eq 17). Because $v_X(x) = -v_H(x)/2$, we may also extract the correlation potential alone $v_c(x)$. From the conditional probability amplitude 6, we construct $v_{xc}^{hole}(x)$ according to eq 7.

The exact KS potential is plotted at several different internuclear distances in Figure.(2) alongside the external potential and the density. As the molecule dissociates, steplike and peaklike features clearly develop in the KS potential. There is a build-up in the KS potential around the more electronegative atom that, at each R, eventually returns to zero on the right-hand side of the atom (one sees the beginning of the return to zero at the smaller separations shown, but at separation $R = 10.0$, this occurs beyond the region plotted).

These features occur in the response and kinetic components of the correlation potential, as is evident in Figure 3. Here, we plot the xc potential (solid), which is the sum of the xc-hole potential (dotted) and the response components $v_{c, kin} + v_{resp}$ (dashed). At equilibrium bond-length ($R = 1.6$ au), the xc potential is dominated by the potential of the xc hole. As the molecule dissociates the $v_{c, kin} + v_{resp}$ components become large giving rise to clear peak and step structures. At large separation, the local variation of the total xc potential around each atom is almost entirely caused by the xc hole: at $R = 6.0$ au and 10.0 au, v_{xc} and v_{xc}^{hole} exactly coincide near Li, while near H they have the same shape, but the well in v_{xc} is translated upward by exactly 3.0 au relative to v_{xc}^{hole}, which is the magnitude of the step ΔI (see section II). At $R = 6.0$ au, the step has reached its asymptotic value of $I_H - I_{Li} = 3.0$ au. As the molecule is pulled apart further, the step does not increase in size, but becomes flatter and larger in spatial extent. In section IVA, we show that the bond-length at which the step begins to develop is related to the position of the avoided crossing between the ground-state and the state that eventually becomes the lowest charge-transfer state.

A sharp peak near the rise of the step is evident in the xc potential (Figure 3); this occurs in the kinetic component to the correlation potential, $v_{c,kin}$, as discussed in section II. We return to an analysis of its magnitude and location in the widely separated limit and an explanation of its role in achieving the exact density of the interacting system in section IVB.

In Figure 4, we plot the potentials for the separation $R = 10.0$. This is the largest separation for which we could converge our numerical method. In the limit of very large separation, we expect that the KS potential reduces simply
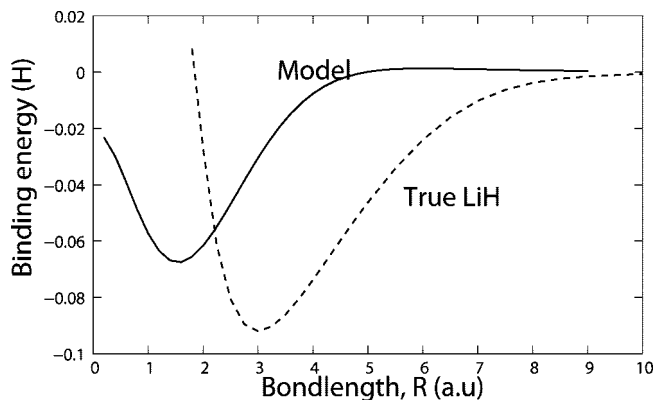

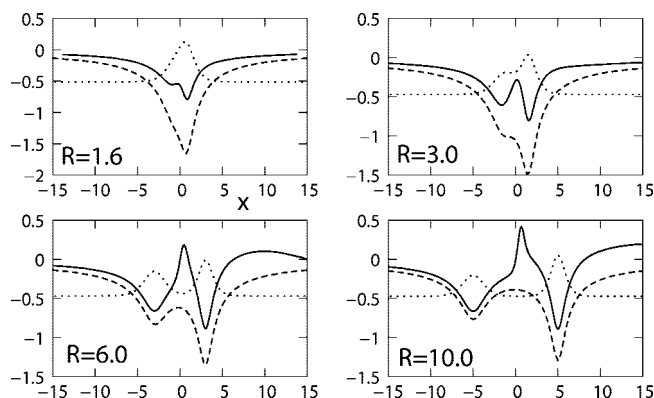**Figure 1.** Binding energy for (1) model 1D LiH and (2) true 3D LiH.

Figure 2. v_S (solid curves), v_{ext} (dashed), and the density (dotted curves) plotted at the internuclear separations indicated.
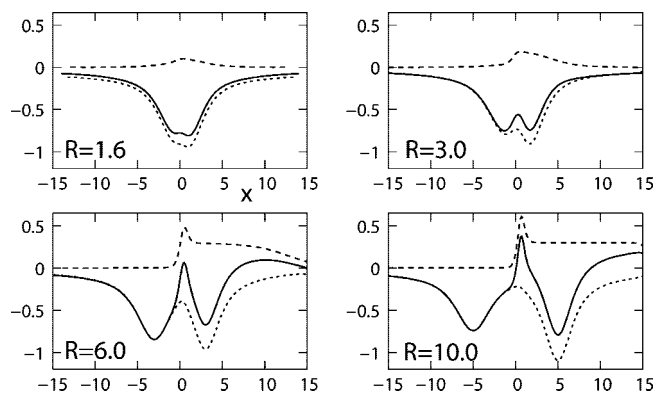

Figure 3. Total xc potential v_{xc} (solid curves), $v_{c,kin} + v_{resp}$ (dashed curves), v_{xc}^{hole} (dotted curves) at various internuclear separations.

to the external potential in the region of the nuclei because it would be a one-electron system around each nucleus. There may be a possible shift up or down relative to the external potential because constants in potentials have no physical relevance. That is, we expect the Hartree-plus-xc potential becomes flat in the atomic regions. We notice in our model at $R = 10.0$, that this is approximately true: there is however a gentle slope in v_{Hxc}, upward around the left nucleus, and downward on the right, and this is largely the result of a Hartree effect. Compared to the atomic densities in true Coulomb-interacting systems, the soft-Coulomb densities in
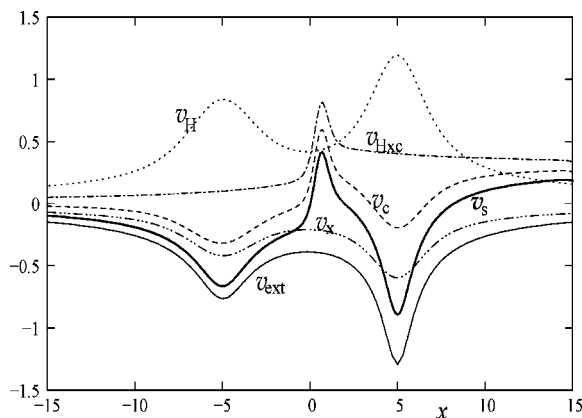
Molecular Dissociation in DFT

J. Chem. Theory Comput., Vol. 5, No. 4, 2009 **775**

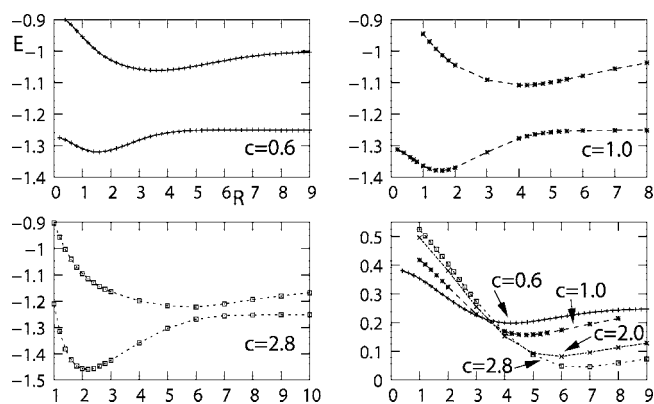**Figure 4.** Components of the potentials for $R = 10.0$.

Figure 5. Ground-state and first-excited state (charge-transfer) potential energy surfaces for our model with $c = 0.6$ (top left), $c = 1.0$ (top right), $c = 2.8$ (bottom left). The energy differences between the surfaces are shown in the bottom right figure; their minimum lies at the avoided crossing.
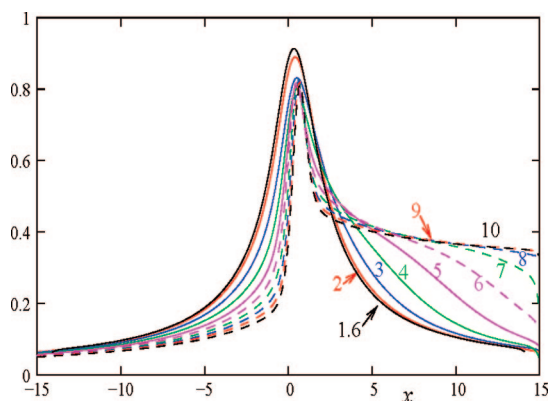

Figure 6. Hartree-exchange-correlation potential, $v_{Hxc}(x)$ for our LiH model ($c = 0.6$); the values of interatomic separation R are indicated.

Figure 7. Hartree-exchange-correlation potential, $v_{Hxc}(x)$ for our LiH model ($c = 2.8$); the values of interatomic separation R are indicated.

Figure 8. Kinetic and response components of the correlation potential $v_{c,kin} + v_{c,resp}$ for our model with $c = 0.6$; the values of interatomic separation R are indicated.

Figure 9. Kinetic and response components of the correlation potential $v_{c,kin} + v_{c,resp}$ for our model with $c = 2.8$.

one-dimension fall off much slower away from their nuclei, resulting in a longer-ranged Hartree and xc potential than in the true 3D counterpart. It is clear from the graph that the Hartree potential is still significant in the interatomic region. In addition to long-ranged correlation effects from the density on the "other" atom (i.e., the peak and step), the xc potential must cancel the local Hartree potential: the exchange potential takes care of half of this cancelation (eq 14), but the correlation potential must also contribute a well of half
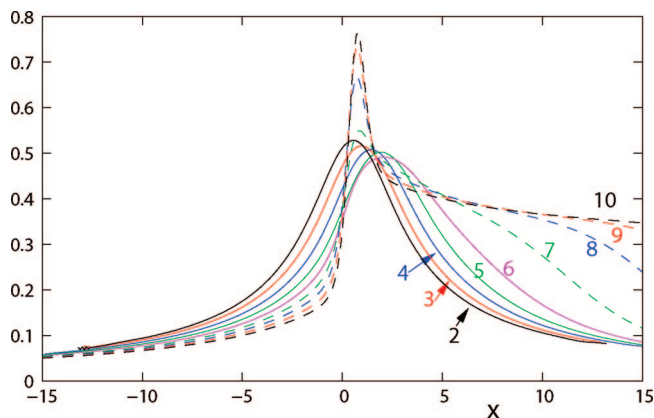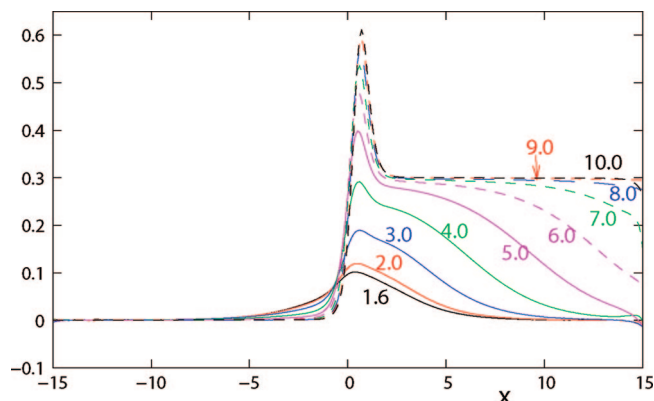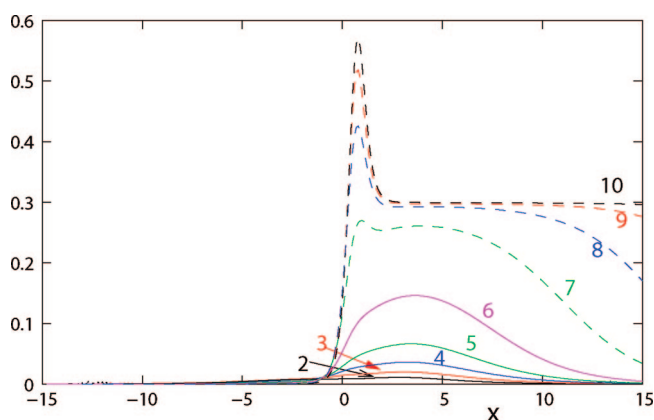
the size of the Hartree, as is evident in the graph. Despite the long-rangedness of the Hartree potential, $R = 10.0$ can still be viewed as "asymptotic" from the point of view of the peak and step structures in the correlation potential: the graph shows clearly that the potential on the hydrogen nucleus on the right is raised by ΔI, and the peak has a height of about 0.76 (see last section).

A. Onset of the Step: Relation to Potential Energy Surface Crossings. We now show that the bond-length at which the step begins to significantly develop is correlated
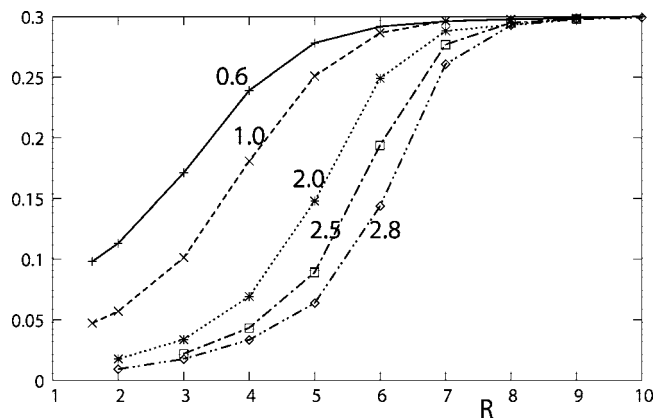
Figure 10. Value of $v_{c\,kin} + v_{resp}$ at the location of the H atom in our model, as a function of the internuclear separation R, and with c-values as indicated.
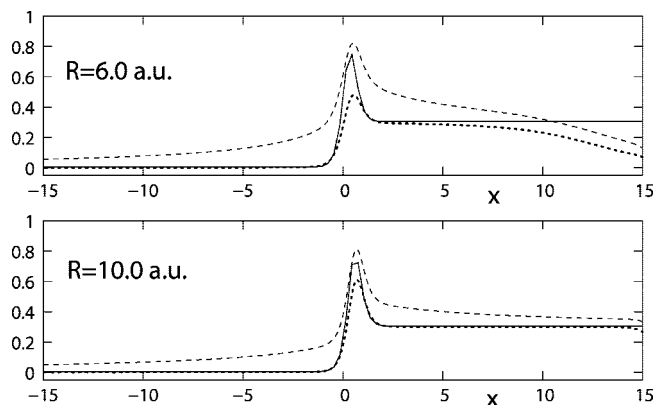

Figure 11. Asymptotic expression for v_{Hxc} (solid curve) in the interatomic region compared to v_{Hxc} in our model (dashed curve), and $v_{kin} + v_{resp}$ (dotted line) in our model at separations indicated.
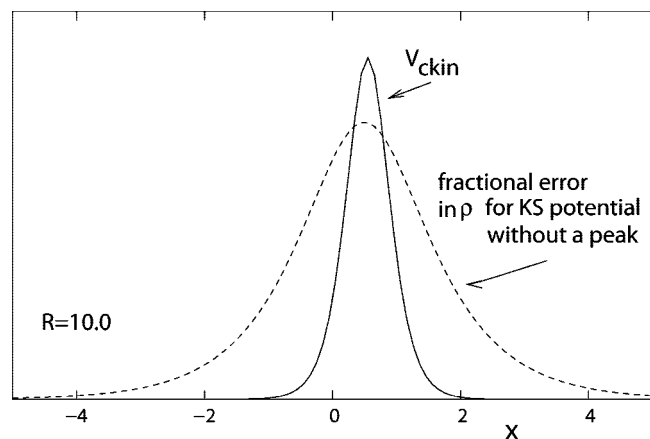

Figure 12. Peak in $v_{c\,kin}(x)$ and that in the fractional density-error of the KS orbital solution to the KS potential with the peak taken out, $\sqrt{(\rho_H\rho_{Li})}/(\rho_H + \rho_{Li})$, (see text) have the same location.

with the position of the avoided crossing in the potential energy surfaces associated with the ground-state and the lowest excited charge transfer state. In a diabatic picture, ionic and covalent curves cross at an internuclear distance, R_C, which is approximately equal to $1/(I_D - A_A)$, where I_D is the ionization energy of the donor and A_A the electron
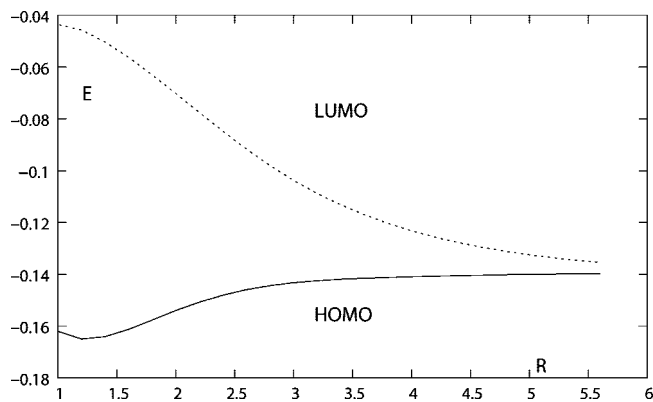

Figure 13. LSD KS eigenvalues for LiH become near-degenerate as a function of internuclear separation R.

affinity of the acceptor, in the lowest charge-transfer state of the long-range molecule.[45] When one considers the adiabatic potential energy surfaces, the crossing becomes an avoided one, whose splitting exponentially decreases as a function of R_C.[45]

What has not been previously pointed out, however, is that the step structure in the KS potential begins to develop in the vicinity of the avoided crossing. Why this must be so lies in the fact that the step is an asymptotic feature, that arises once the two atoms are independent systems, and its shift of the eigenvalues of the more tightly bound atom ensures that the ground-state solution of the KS potential has exactly half the density (i.e., one electron) on either side of the midpoint (see section II). The development of the step must therefore track the independence of the two atomic systems (measured, for example, by their indifference to a perturbation on the other atom). The avoided crossing marks the point at which the molecule transitions (moving from short bond distances to longer ones) from a single system to two independent systems. The width of this transition tracks the magnitude of the ground-excited energy gap at the avoided crossing, that is, it should be wider when the avoided crossing is at small bond distances and sharper when the avoided crossing occurs at large distances.

Our model demonstrates this explicitly. Figure 5 presents the ground- and first excited-state potential energy surfaces for three different values of the electron−electron soft-Coulomb parameter, c. As c increases, the avoided crossing moves out and becomes sharper; the lowest-energy gap therefore decreases, indicating that the transition from ionic to covalent character occurs more abruptly.

In Figure 6, we plot the Hartree plus xc potential, $v_{Hxc}(x)$ $= v_H(x) + v_{xc}(x)$ for a range of internuclear separations R, for $c = 0.6$. Because this is the net potential that gets added to the external potential, we expect that in the limit of wide separation, it becomes flat around each nucleus because it should describe essentially two one-electron systems. We see this in the graph, where a definite step is visible from $R = 5.0$ and higher. We see that it is indeed in the approach to the avoided crossing, at about $R = 4.0$, that a shoulder first becomes clearly visible around the atom with the higher IP; this develops fully into a step of size ΔI, as the molecule dissociates.

Molecular Dissociation in DFT

J. Chem. Theory Comput., Vol. 5, No. 4, 2009 **777**

In Figure 7, we plot v_{Hxc} for $c = 2.8$. The step begins to develop at larger R, corresponding to the larger R_C where the avoided crossing occurs. Also, as the avoided crossing becomes sharper, the onset of the step happens more rapidly.

The long-rangedness of the density in soft-Coulomb systems means that the Hartree and exchange terms decay slower than in the usual Coulomb case. To clarify the step and peak structures, we plot just the kinetic plus response term in Figure 8 for our LiH model of $c = 0.6$ and in Figure 9 for $c = 2.8$. The relation between the R at which the step develops and the avoided crossing discussed above is seen more clearly in these figures. Finally, in Figure 10, we plot the value of $v_{c,kin} + v_{resp}$ at the location of the atom with the larger IP (the H atom in our model), as a function of internuclear separation R, for various different c-values. This graph shows quite clearly that the development of the step tracks the location and sharpness of the avoided crossing: the larger the separation at which the avoided crossing occurs (i.e., larger c-value), the consequently larger R the step is onset and that the step develops more sharply, corresponding to the sharper avoided crossing at larger distances.

B. Asymptotic Separation Limit, and the Significance of the Peak. Analytic expressions for the xc potential and its components in our two-electron model can be found in the separated-atom limit, by adopting the Heitler−London form for the wave function

$$\Phi_{HL}(x, x') = \frac{\phi_H(x)\phi_{Li}(x') + \phi_{Li}(x)\phi_H(x')}{\sqrt{2(1 + S_{H,Li}^2)}} \quad (21)$$

where $S_{H,Li}$ is the overlap integral

$$S_{H,Li} = \int \phi_H(x)\phi_{Li}(x)dx \quad (22)$$

We will focus on the interatomic region, far from either nuclei, in this limit. To lowest order in the separation R, the orbitals $\phi_{Li}(x)$ and $\phi_H(x)$ in this region may be written

$$\begin{align} \phi_H(x) &= \sqrt{\alpha_H}e^{\alpha_H(x - \frac{R}{2})} \\ \phi_{Li}(x) &= \sqrt{\alpha_{Li}}e^{-\alpha_{Li}(x + \frac{R}{2})} \end{align} \quad (23)$$

where $\alpha = \sqrt{(2I)}$, with I being the first ionization potential of the atom. Similar expressions hold for the three-dimensional case, with Coulomb interaction; the only differences being that instead the orbitals have asymptotic dependence according to

$$\phi(x) = \alpha^{3/2}e^{-\alpha[(x \pm (R/2))^2 + y^2 + z^2]^{1/2}} \quad (24)$$

(where the x-axis is taken to be the bond axis).

It is a simple exercise to construct the first-order density-matrix and the density using these orbitals. Substituting into eqs 12 and 9 yields the large-separation limit of the KS potential and $v_{kin}(r)$.

In the limit of large interatomic separation, the Hartree potential vanishes as the inverse distance from the nuclei in the interatomic region. Also, in this limit, the second-order density matrix factorizes into a product of densities and it follows from eq 5 that $v_{xc}^{hole}(r)$ also falls off as the inverse

distance from the nuclei in the interatomic region. The KS potential is then dominated by contributions from $v_{kin}(r)$ and $v_{resp}(r)$. Explicitly, in one dimension, this is given by

$$\begin{align} v_S &= \frac{1}{2}\frac{|\phi'_H|^2 + |\phi'_{Li}|^2 + 2\sqrt{\epsilon}(\phi'_H)(\phi'_{Li})}{|\phi_H|^2 + |\phi_{Li}|^2 + 2\sqrt{\epsilon}\phi_H\phi_{Li}} + \\ &\quad \frac{1}{2}\frac{\phi_H\phi''_H + \phi_{Li}\phi''_{Li} + \sqrt{\epsilon}(\phi_{Li}\phi''_H + \phi_H\phi''_{Li})}{|\phi_H|^2 + |\phi_{Li}|^2 + 2\sqrt{\epsilon}\phi_H\phi_{Li}} - \\ &\quad \frac{1}{4}\frac{(\phi_H\phi'_H + \phi_{Li}\phi'_{Li} + \sqrt{\epsilon}(\phi_{Li}\phi'_H + \phi_H\phi'_{Li})^2}{(|\phi_H|^2 + |\phi_{Li}|^2 + 2\sqrt{\epsilon}\phi_H\phi_{Li})^2} - I_{Li} \quad (25) \end{align}$$

In the above expression, ϕ' and ϕ'' denote the first and second spatial derivatives of the orbital, and ϵ is the square of the overlap integral at interatomic separation R

$$\epsilon = \frac{\alpha_H\alpha_{Li}}{(\alpha_H - \alpha_{Li})^2}(e^{-R\alpha_{Li}} - e^{-R\alpha_H})^2 \quad (26)$$

In Figure 11), the asymptotic expression for $v_{Hxc}(= v_S - v_{ext})$ using the orbitals of eq 23 is plotted for comparison with the $v_{c,kin}(r) + v_{resp}(r)$ component of the numerical solution using the soft-Coulomb potentials. (As noted earlier, the soft-Coulomb orbitals are longer-ranged than their 3D Coulomb counterparts, so v_{Hxc} achieves its asymptotic form only at larger distances.) We see that the step reaches its asymptotic limit more quickly than the peak. For instance, at $R = 10.0$ au the peak for the numerical solution is somewhat smaller than that of the analytic expression, although the step has already reached its asymptotic value of 3.0H.

We next derive asymptotic expressions for the location and magnitude of the peak and step structures as functions of the internuclear separation. Defining the location of the peak from the condition $(d/dx)v_{c,kin}|_{x_{peak}} = 0$, we obtain

$$x_{peak} = \frac{R}{2}\frac{\left(1 - \sqrt{\frac{I_{Li}}{I_H}}\right)}{\left(1 + \sqrt{\frac{I_{Li}}{I_H}}\right)} + \frac{1}{\sqrt{32}}\frac{\ln\frac{I_{Li}}{I_H}}{\sqrt{I_{Li}} + \sqrt{I_H}} \quad (27)$$

where I_{Li} and I_H are the ionization potentials of Li and H, respectively. For the 3D case, the second term on the right is modified to be

$$\frac{3}{\sqrt{32}}\frac{\ln\frac{I_{Li}}{I_H}}{\sqrt{I_{Li}} + \sqrt{I_H}} \quad (28)$$

Defining the location of the step by its inflection point, that is, from the condition $(d^2/dx^2)v_{resp} = 0$, one obtains the same result, that is,

$$x_{step} = x_{peak} \quad (29)$$

Therefore, in the asymptotic limit, our two-electron model shows that the location of the peak and step coincide. The second term in eq 27 is negative, but in general small

compared to the first term for large interatomic separation R. Therefore, the peak and step structures are located closer to the hydrogen atom, more generally, closer to the more electronegative atom of a diatomic molecule. On the other hand, the minimum of the density

$$x_{\min(n)} = \frac{R}{2}\frac{\left(1 - \sqrt{\frac{I_{Li}}{I_H}}\right)}{\left(1 + \sqrt{\frac{I_{Li}}{I_H}}\right)} + \frac{1}{\sqrt{32}}\frac{\ln\frac{I_{Li}^2}{I_H^2}}{\sqrt{I_{Li}} + \sqrt{I_H}} \qquad (30)$$

lies closer to Li than the peak/step location, but still on the side of the bond midpoint closer to H: The first term of eq 30 is identical to eq 27, while the second term contains the logarithm of the ratio I_{Li}^2/I_H^2 instead of the ratio I_{Li}/I_H, which is smaller than one.

Our simple two-electron model thus explains the earlier observations in real molecules:[19] In the general many-electron heteroatomic case, given that the peak and step structures arise from the delocalized HOMO, our analysis can predict their positions. The location of the step was seen to coincide with the peak in the true LiH molecule, with both lying closer to the H atom, at least for the largest interatomic distances that those calculations were able to perform. For the homoatomic case, our results (eqs 27 and 30) predict that $x_{peak} = x_{\min(n)} = 0$, and so, the minimum of the density and peak location coincide at the bond midpoint; also borne out by the examples in the literature.

We next turn to the magnitudes of the structures. Using the density matrix constructed from the orbitals in eq 23, one can show that the magnitude of the peak structure in $v_{kin}(r)$, in the limit that the overlap integral vanishes, is given by the expression

$$v_{c,kin}^{max} = \frac{1}{4}\left(\sqrt{I_H} + \sqrt{I_{Li}}\right)^2 \qquad (31)$$

For our two-electron model of LiH, this gives a value of 0.616 au. Adding the value of the step in v_{resp} at its inflection point ($\Delta I/2 = 0.15$ au), gives 0.7672 au, which is indeed the peak to which our numerical solution asymptotes. For the homoatomic case, the above expression gives a value of $V_{peak} = 0.5$ au, agreeing with the results of ref 19 and16 for the true homoatomic two electron system H_2. However, in ref 19, the magnitude of the peak for *true* LiH, was significantly smaller than this prediction. This discrepancy is due to the effect of the localized core electrons in the Li 1s shell, which lead to a dramatic decrease in the magnitude of the gradient of the conditional probability amplitude eq 6 in the interatomic region, and hence by eq 9, a decrease in the magnitude of the peak.

As discussed in section II, the peak emerges out of analyzing the change in the conditional probability. We now give a different argument for why the peak must be there, even though it has negligible effect on the ground-state energetics. The peak occurs when one takes the "nonbonding" orbital as the KS orbital

$$\phi = \sqrt{(\rho_H + \rho_{Li})/2} \qquad (32)$$

(Here ρ_H is the atomic density of the H atom and ρ_{Li} that of the Li atom, that is, the squares of the orbitals in eq 23). This is the exact doubly occupied KS orbital, since twice its square yields the exact density in the limit of infinite separation, $\rho = 2|\phi|^2 = \rho_H + \rho_{Li}$.

If one instead takes the "bonding orbital"

$$\phi_{bond} = \left(\sqrt{\rho_H/2} + \sqrt{\rho_{Li}/2}\right) \qquad (33)$$

and finds the KS potential corresponding to this, there is *no* peak structure (but there is still the step). That is, if one asks what is the KS orbital for the KS potential with the peak structure sliced out, the KS orbital would instead be ϕ_{bond}. Now the density corresponding to ϕ_{bond} is

$$\rho_{bond} = 2|\phi_{bond}|^2 = \rho_H + \rho_{Li} + 2\sqrt{\rho_H\rho_{Li}} \qquad (34)$$

that is, is equal to the sum of the atomic densities *plus* a term $2\sqrt{(\rho_H\rho_{Li})}$. This term is indeed very small, but taken as a fraction of the total density, $(\rho_H\rho_{Li})^{1/2}/(\rho_H + \rho_{Li})$, displays a peak at the exact same location as the peak in the *exact* KS potential, eq 27 (Figure 12). The shape of the peak is different but its maximum coincides in the limit of infinite separation. This suggests an interpretation of the peak in $v_{c,kin}$ (in the exact KS potential), as a barrier that pushes back to the atomic regions the extraneous density $2\sqrt{(\rho_H\rho_{Li})}$ that would be in the bonding region if the peak was absent. Since the KS system by definition must get the density correct the peak must be there.

The interpretation here is closely related to the analysis of ref 21 of homoatomic molecules, where it was shown that the kinetic energy density for the exact KS orbital develops a well in the bond midpoint region, that must be compensated by a peak in the KS potential to keep the constant value of the KS orbital energy. An LCAO approximation to the orbital (analogous to ϕ_{bond} above) does not display the well.

V. Discussion and Implications

Using a simple one-dimensional model of a two-electron heteroatomic molecule, we studied features of the exact KS potential that arise for real 3D heteroatomic molecules. In particular, we examined the characteristic step and peak structure in the internuclear region, which develop as the molecule dissociates. These unusual features are a peculiarity of the noninteracting KS description: on the one hand, as a molecule dissociates, the interaction between the electrons on one atom and those on the other vanishes, so why, fundamentally, do such stark structures appear in the KS potential? The answer ultimately lies in the single-Slater-determinant description in the KS system: although this is indeed how the exact KS system describes the state, it is far from the true wave function which needs, even qualitatively, two Slater determinants. In the two-electron model, the KS system consists of a doubly occupied spatial orbital, blatantly far from the true two-orbital interacting system. Mathematically, the structures can be understood by considering the response and kinetic components of the correlation potential,

Molecular Dissociation in DFT

J. Chem. Theory Comput., Vol. 5, No. 4, 2009 **779**

as explained in earlier works and in Section II of the present paper. Physically, a KS potential that lacks the step leads to dissociation into fractional charges; a KS potential that lacks the peak leads to a KS orbital that yields an incorrect (albeit exponentially small) density in the internuclear region. The former point is well-recognized in the literature, while the latter point elaborates on an earlier interpretation[21] (section IVB).

Because of the simplicity of our two-electron model, we are able to investigate in much more detail than in the earlier literature, the development of these structures and their asymptotic properties. Several of these features carry over to the true many-electron 3D case, since they arise from the HOMO orbital. We showed that the step begins to develop at the internuclear separation, where the avoided crossing in the ground and lowest charge-transfer state is approached, and explained why. We gave an exact formula for the location of the step and peak, in the limit of large separation, finding that the two structures are located at the same place, and closer to the atom with the larger IP, consistent with the few calculations done on real molecules in the literature.

Because they are in a region of very low electron-density, these features, in themselves, have little energetic consequences for the ground states of these systems. However they have dramatic consequences for time-dependent processes, excitations, and response. For example, it has been shown that the related peaks that appear in the interatomic regions of a hydrogen chain significantly (and correctly) reduce the polarizability of the chain and that local and semilocal approximations which lack the peak, consequently significantly underestimate the (hyper-)polarizability.[35] As TDDFT begins to be utilized in molecular transport calculations, we anticipate the peaks will act as barriers decreasing the current.

The step in the KS potential ultimately imposes a rather complicated structure on the exact xc kernel of TDDFT.[37,38] Because of the realignment of the atomic HOMOs, the molecular HOMO and LUMO are symmetric and antisymmetric combinations of the atomic HOMO's, separated in energy merely by the tunnelling factor, that vanishes as $\exp(-\text{const } R)$ as the molecule dissociates. Therefore three KS determinants become near-degenerate: the doubly occupied HOMO, a single-excitation to the LUMO, and a double-excitation to the LUMO. That is, the step introduces *static correlation* in the KS system that is not present in the true interacting system. It is the job of the TDDFT xc kernel to "undo" this static correlation, in order to yield good excitation energies in the true system. This has a dramatic effect on the structure of the xc kernel for charge-transfer excitations in molecules composed of open-shell fragments;[37,38] in particular, the double-excitation induces a strong-frequency-dependence on the kernel.

Almost all the approximations in use today do not capture the step and peak structure in the potential. Carefully constructed orbital functionals for the correlation potential may display these structures, as has been explicitly shown in ref 46. Interestingly, static correlation in the KS system is nonetheless not escaped in the usual (semi)local approximations. Delocalized orbitals underlie the fractional charge problem, and the HOMO and LUMO become near-degenerate as the molecule dissociates. Figure 13 demonstrates this for the LiH molecule within LSD; a similar merging of the HOMO and LUMO is also seen in GGA.

References

(1) Hohenberg, P.; Kohn, W. *Phys. Rev.* **1964**, *136*, B 864.

(2) Kohn, W.; Sham, L. J. *Phys. Rev.* **1965**, *140*, A 1133.

(3) Kohn, W. *Rev. Mod. Phys.* **1999**, *71*, 1253.

(4) Perdew, J. P.; Kurth, S. Density Functionals for Non-Relativistic Coulomb Systems in the New Century. In *A Primer in Density Functional Theory*; Fiolhais, C., Nogueira, F., Marques, M., Eds.; Springer: Berlin, Heidelberg, New York, 2003; Vol. 620, pp 1−55.

(5) *A Primer in Density Functional Theory*; Springer Lecture Notes in Physics 620; Fiolhais, C., Nogueira, F., Marques, M., Eds.; Springer: Berlin, Heidelberg, New York, 2003.

(6) Perdew, J. P.; Burke, K.; Ernzerhof, M. *Phys. Rev. Lett.* **1996**, *77*, 3865.

(7) Staroverov, V. N.; Scuseria, G. E.; Tao, J.; Perdew, J. P. *J. Chem. Phys.* **2003**, *119*, 12129.

(8) Staroverov, V. N.; Scuseria, G. E.; Tao, J.; Perdew, J. P. *J. Chem. Phys.* **2004**, *121*, 11507(E).

(9) Rydberg, H.; Dion, M.; Jacobson, N.; Schroder, E.; Hyldgaard, P.; Simak, S. I.; Langreth, D. C.; Lundqvist, B. I. *Phys. Rev. Lett.* **2003**, *91*, 126402.

(10) Cooper, V. R.; Thonhausr, T.; Langreth, D. C. *J. Chem. Phys.* **2008**, *128*, 204102.

(11) Vydrov, O. A.; Wu, Q.; van Voorhis, T. *J. Chem. Phys.* **2008**, *129*, 014106.

(12) Slater, J. C. *The Self-Consistent Field for Molecules and Solids*; McGraw-Hill: New York, 1974.

(13) Perdew, J. P.; Parr, R. G.; Levy, M.; Balduz, J. L. *Phys. Rev. Lett.* **1982**, *49*, 1691.

(14) Perdew, J. P. What do the Kohn-Sham orbitals mean? How do atoms dissociate? In *Density Functional Methods in Physics*; Dreizler, R. M., da Providencia, J., Eds.; Plenum: New York, 1985; p 265.

(15) Ruzsinszky, A.; Perdew, J. P.; Csonka, G. I.; Vydrov, O. A.; Scuseria, G. E. *J. Chem. Phys.* **2006**, *125*, 194112.

(16) Buijse, M. A.; Baerends, E. J.; Snijders, J. G. *Phys.Rev. A.* **1989**, *40*, 4190.

(17) Gritsenko, O. V.; van Leeuwen, R.; Baerends, E. J. *Phys.Rev. A.* **1995**, *52*, 1870.

(18) Gritsenko, O. V.; van Leeuwen, R.; Baerends, E. J. *J. Chem. Phys.* **1996**, *104*, 8535.

(19) Gritsenko, O. V.; Baerends, E. J. *Phys.Rev. A.* **1996**, *54*, 1957.

(20) Gritsenko, O. V.; van Leeuwen, R.; Baerends, E. J. *J. Chem. Phys.* **1994**, *101*, 8955.

(21) Gritsenko, O. V.; Baerends, E. J. *Theor. Chem. Acc.* **1997**, *96*, 44.

(22) van Leeuwen, R.; Baerends, E. J. *Phys. Rev. A.* **1994**, *49*, 2421.

(23) Runge, E.; Gross, E. K. U. *Phys. Rev. Lett.* **1984**, *52*, 997.

(24) Petersilka, M.; Gossmann, U. J.; Gross, E. K. U. *Phys. Rev. Lett.* **1996**, *76*, 1212.

(25) *Time-Dependent Density Functional Theory*; Marques, M. A. L., Ulrich, C. A., Nogueira, F., Rubio, A., Burke, K., Gross, E. K. U., Eds.; Springer: Berlin, 2006.

(26) Levine, B. G.; Ko, C.; Quenneville, J.; Martinez, T. J. *Mol. Phys.* **2006**, *104*, 1039.

(27) Javanainen, J.; Eberly, J.; Su, Q. *Phys. Rev. A.* **1988**, *38*, 3430.

(28) Eberly, J.; Grobe, R.; Law, C.; Su, Q. In *Atoms in Intense Laser Fields*; Gavrila, M., Ed.; Academic Press: Boston, 1992.

(29) Villeneuve, D. M.; Ivanov, M. Y.; Corkum, P. B. *Phys. Rev. A.* **1996**, *54*, 736.

(30) Bandrauk, A.; Ngyuen, H. *Phys. Rev. A.* **2002**, *66*, 031401(R).

(31) Bandrauk, A.; Lu, H. *Phys. Rev. A.* **2005**, *72*, 023408.

(32) Lein, M.; Gross, E. K. U.; Engel, V. *Phys. Rev. Lett.* **2002**, *85*, 4707.

(33) Ngyuen, H.; Bandrauk, A. *Phys. Rev. A.* **2006**, *73*, 032708.

(34) Lein, M.; Kümmel, S. *Phys. Rev. Lett.* **2005**, *94*, 143003.

(35) Kümmel, S.; Kronik, L.; Perdew, J. P. *Phys. Rev. Lett.* **2004**, *93*, 213002.

(36) Koentopp, M.; Chang, C.; Burke, K.; Car, R. J. *Phys. Cond. Matt.* **2008**, *20*, 083203.

(37) Maitra, N. T. *J. Chem. Phys.* **2005**, *122*, 234104.

(38) Maitra, N. T.; Tempel, D. G. *J. Chem. Phys.* **2006**, *125*, 184111.

(39) Almbladh, C. O.; von Barth, U. *Phys. Rev. B.* **1985**, *31*, 3231.

(40) Perdew, J. P.; Levy, M. *Phys. Rev. B.* **1997**, *56*, 16021.

(41) Boutalib, A.; Gadea, F. X. *J. Chem. Phys.* **1992**, *97*, 1144.

(42) Castro, A.; Appel, H.; Oliveira, M.; Rozzi, C. A.; Andrade, X.; Lorenzen, F.; Marques, M. A. L.; Gross, E. K. U.; Rubio, A. *Phys. Status Solidi B* **2006**, *243*, 2465–2488.

(43) Marques, M. A. L.; Castro, A.; Bertsch, G. F.; Rubio, A. *Comput. Phys. Commun.* **2003**, *151*, 60–2003.

(44) http://www.tddft.org/programs/octopus/wiki/index.php/MainPage (accessed 2008).

(45) Grice, R.; Herschbach, D. R. *Mol. Phys.* **1972**, *27*, 159.

(46) Gritsenko, O. V.; Baerends, E. J. *Int. J. Quantum Chem.* **2006**, *106*, 3167.

CT800535C